

## GAMMA-RAY SPECTROSCOPY OF SOME Pd ISOTOPES PRODUCED IN INDUCED FISSION REACTIONS

STEPHANE LALKOVSKI, ANI MINKOVA, STOYANKA ILIEVA

*Department of Atomic Physics*

*Стефан Лалковски, Ани Минкова, Стоянка Илиева. ГАМА СПЕКТРОСКОПИЯ НА НЯКОИ ПАЛАДИЕВИ ИЗОТОПИ, ПОЛУЧЕНИ В РЕАКЦИИ НА ИНДУЦИРАНО ДЕЛЕНЕ*

Тази статия разглежда реакциите на сливане с делене и процеса на делене, индуциран от тежки йони. В детайли е обяснено приложението на  $\gamma$ -спектроскопията на фрагменти на делене на базата на няколко Pd изотопи, получени в реакция  $^{176}\text{Yb} + ^{31}\text{P}$  при енергия на снопа 152 MeV.

*Stephane Lalkovski, Ani Minkova, Stoyanka Ilieva. GAMMA-RAY SPECTROSCOPY OF SOME Pd ISOTOPES PRODUCED IN INDUCED FISSION REACTIONS*

This article gives an overview on the fusion/fission reactions and the fission process induced by heavy ions. The application of  $\gamma$ -ray fission fragment spectroscopy is explained in details on the basis of some Pd isotopes obtained in the reaction  $^{176}\text{Yb} + ^{31}\text{P}$  at 152 MeV beam energy.

**Keywords:** level energies;  $\gamma$  transitions; fusion/fission reactions;  $\gamma$ -ray spectroscopy

**PACS number:** 21.60.n; 23.20.Lv; 25.70.Jj; 27.60.+j

### 1. INTRODUCTION

There are several mechanisms for population of high-spin states: fusion/evaporation reactions, fusion/fissions reactions and spontaneous fission. The fusion/evaporation reactions give access to the neutron deficient side of the chart of nuclides and the spontaneous fission populates the extremely neutron-rich side but there remains a not well explored area of nuclei with enough neutrons. The only way

to populate nuclei in this area before the radioactive beams to become available is through induced fission. Moreover, using fusion/fission reaction by appropriate combination of target and beam we may access different regions of the chart of nuclides.

Palladium isotopes of  $A \approx 108-110$  are in the region of intermediate number of neutrons and the only way to populate them is by fusion/fission reactions. Why are we interested in these Pd isotopes? The high-spin studies of the lighter Pd isotopes ( $A \leq 106$ ) using fusion/evaporation reactions has contributed greatly to the understanding of the collective properties of these transitional nuclei. High-spin states in the heavier Pd isotopes have been investigated only recently when the large multidetector arrays became available for experiments. The extended level schemes of Pd isotopes 108 and 110 would confirm or not the predicted shape transition in this mass area.

## 2. HEAVY ION REACTIONS

At low energies two heavy ions interact through their Coulomb fields. Nuclear interaction takes place when the two-ion energy in center-of-mass system  $E_{cm}$  is high enough to overcome the Coulomb barrier. The reaction mechanism depends

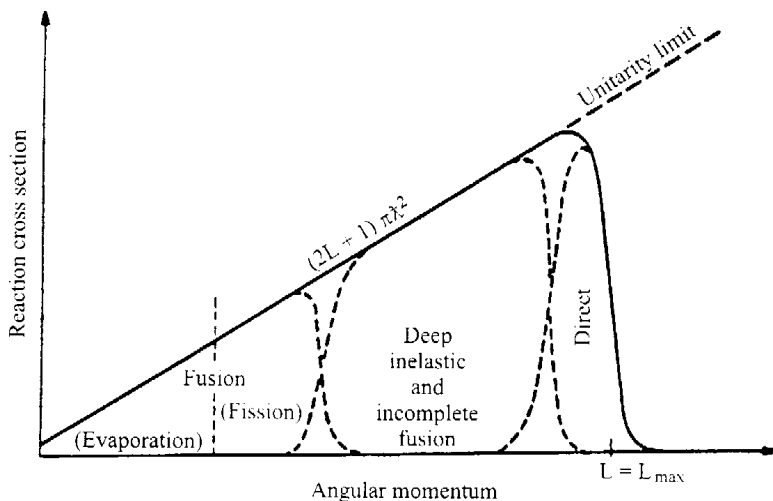


Fig. 1. The reaction cross-section via transferred angular momentum (from ref. [1])

on the transferred angular momentum defined as  $L = m_p v_p b$ . Here  $m_p$  and  $v_p$  are the projectile mass and velocity and  $b$  is the impact parameter. Obviously, only heavy ions of high-energy could have very high angular momentum. There are several competing mechanisms depending on the transferred angular momentum (see Fig. 1).

At low value of the impact parameter, when it is smaller than the distance of closest approach, the most dominant process is the fusion reaction. The projectile and the target form a compound nucleus. After the initial formation of a compound nucleus<sup>1</sup> from the projectile and the target nucleus, the process of equilibration

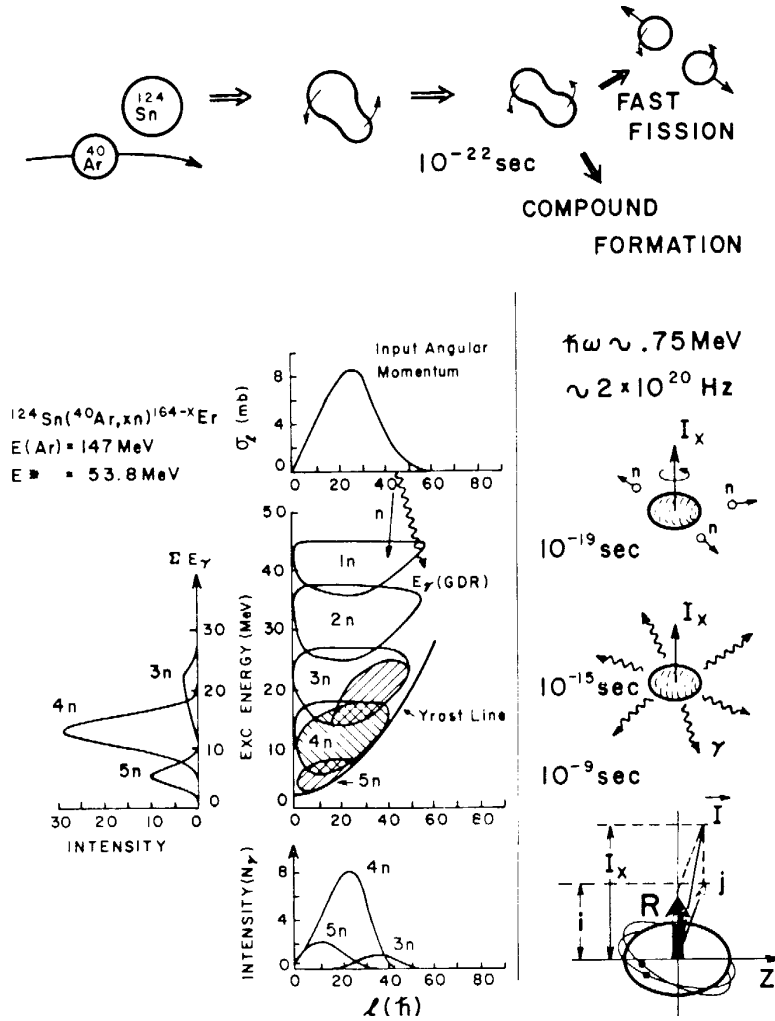


Fig. 2. Fusion/evaporation and fusion/fission competing mechanisms (from ref. [3])

distributes the energy over all nucleons and some of them can be emitted. In general, not only neutrons but also charged particles can be emitted from the

<sup>1</sup>One speaks about the formation of a compound nucleus if the lifetime of the composite system is long enough ( $> 10^{-20}$  s).

highly excited nucleus. The cross-section for pre-equilibrium emission increases with energy, but it is high enough even at energies slightly above the Coulomb barrier. Emission of one neutron lowers considerably the excitation energy of the nuclear system, at least by its separation energy of  $\sim 8\text{--}10$  MeV. The system cools down significantly after emission of 5–7 neutrons, but it still has high angular momentum. The compound nucleus emits a cascade of  $\gamma$ -quanta lowering its energy and angular momentum (Fig. 2).

Once the compound nucleus is formed its angular momentum may be so high that it will be unstable towards nuclear fission. This channel is in a competition with the fusion/evaporation process. The composite system may fission after the initial emission of light particles. The fission fragments are highly excited. Each of them de-excites itself by evaporation of neutrons and after the emission of cascades of  $\gamma$ -quanta they reach their ground states.

The state populated after the emission of the last particle is called entry state (see Fig. 2). The set of all entry states forms entry region. The entry regions are above the yrast line, which is the sequence of states with highest angular momentum for a fixed energy.

The fission probability increases with the angular momentum (Fig. 1). Using the liquid drop model Wilczinski has found that the complete fusion cross section depends on some critical angular momentum  $l_{\text{crit}}$ , i.e., at angular momentum higher than some critical value the fission barrier vanishes and the compound system cannot exist any longer [2]. The cross section for the complete fusion (CF) is given by:

$$\sigma_{\text{CF}} = \pi\lambda^2 \sum_{l=0}^{l_{\text{crit}}} (2l+1)T_l, \quad (1)$$

where  $\lambda^2 = \hbar^2/2\mu E$  and  $T_l$  is the transmission coefficient corresponding to the complete fusion of the target and projectile calculated via the optical model.

The total reaction cross-section can be expressed as

$$\sigma_{\text{R}} = \pi\lambda^2 \sum_{l=0}^{\infty} (2l+1)T_l. \quad (2)$$

Here a sharp cut-off approximation has been assumed:

$$T_l = \begin{cases} 1 & \text{for } l \leq l_{\text{max}} \\ 0 & \text{for } l > l_{\text{max}} \end{cases},$$

where  $l_{\text{max}}$  corresponds to a peripheral collision defined by

$$l_{\text{max}}^2 = \frac{2\mu R^2}{\hbar^2} (E_{\text{cm}} - V_c). \quad (3)$$

Here  $R$  is the maximum distance between the nuclei, at which the collision leads to reaction, and  $\mu$  is the reduced mass of the system.

The Coulomb energy  $V_c$  in eq. (3) is given by

$$V_c = 1.442 \frac{Z_1 Z_2}{R} \quad (4)$$

in units of MeV when  $R$  is in fm and  $Z_1$  and  $Z_2$  are the atomic numbers.

With increasing impact parameter (see Fig. 1) the incomplete fission and deep inelastic collisions are the most dominant processes. In this region both nuclei overlap less than in the case of complete fusion, but their overlapping is still considerable to allow strong interaction between the nuclei. Both nuclei are connected by a neck through which a substantial energy transfer occurs but very few nucleons are transferred from one to another nucleus. When this binuclear system breaks both fragments are similar to the projectile and the target nucleus.

The peripheral collisions are the most dominant processes with the increase of the impact parameter.

### 3. PROPERTIES OF THE FISSION

The measured fission probability is compared to the optical model values in Ref. [4]. It was shown that the fission probability depends on the mass asymmetry of the system projectile-target: it decreases when the mass asymmetry increases. In Fig. 3 the total probability  $P_f = \sigma_f / \sigma_{CF}$  ( $\sigma_f$  is the fission cross-section) is plotted as a function of the excitation energy  $E^*$ . This figure represents the results from the reactions  $^{30}\text{Si} + ^{170}\text{Er}$  and  $^{19}\text{F} + ^{181}\text{Ta}$ . Obviously, when the compound nucleus  $^{200}\text{Pb}$  is produced at the same excitation energy  $E^*$  in both reactions, the probability  $P_f$  for the  $^{30}\text{Si}$  induced reaction is considerably higher than that for reaction induced by  $^{19}\text{F}$ .

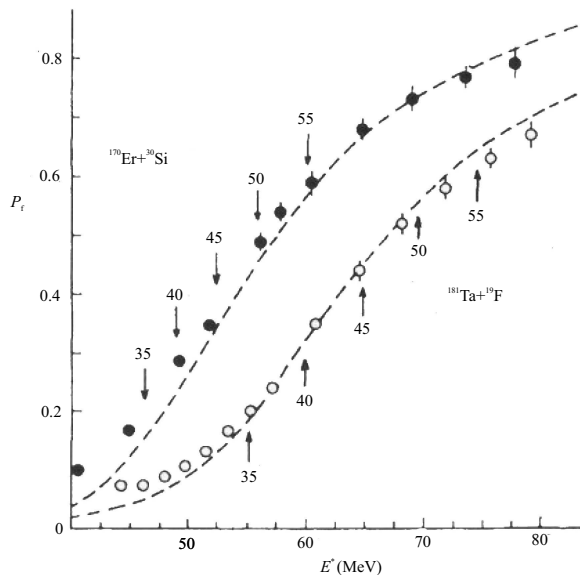


Fig. 3. Total fission probabilities. The vertical arrows indicate maximal angular momentum  $L_{\max}$  (from ref. [4])

In the case of spontaneous fission the fragments are not of equal mass; the fission is then said to be asymmetric. In the case of induced fission the asymmetry in mass decreases with the increase the bombarding energy and fission becomes more and more symmetric. Thus the produced fission fragments have the same  $Z/A$  ratio as the fissioning nucleus.

Figure 4 shows an experimental study of fission fragment mass distribution obtained in deuteron- and  $^{12}\text{C}$ -induced reactions. One can see that the broadening increases with bombarding energy and for Bi+d (190 MeV) it is similar to that corresponding to Au+ $^{12}\text{C}$  (112 MeV) reaction.

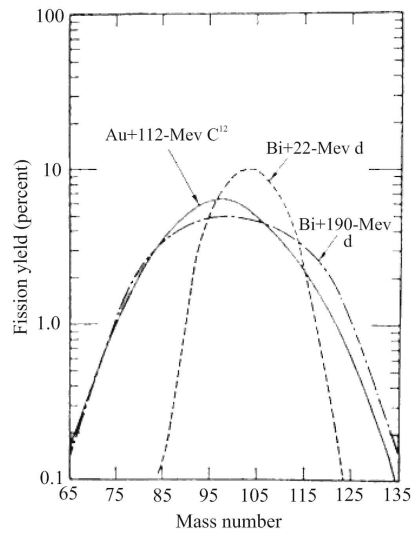


Fig. 4. Fission fragment mass distribution in low-energy induced fission (from ref. [5])

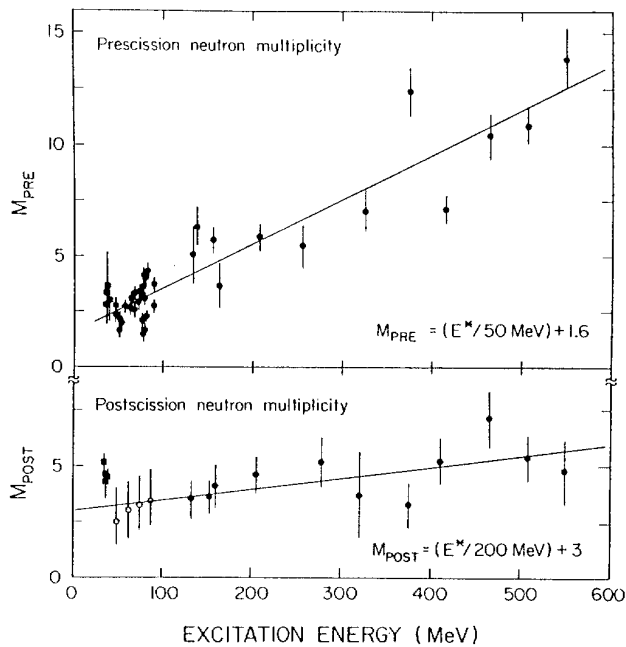


Fig. 5. Neutron multiplicity versus total excitation energy of the compound nucleus (from ref. [5])

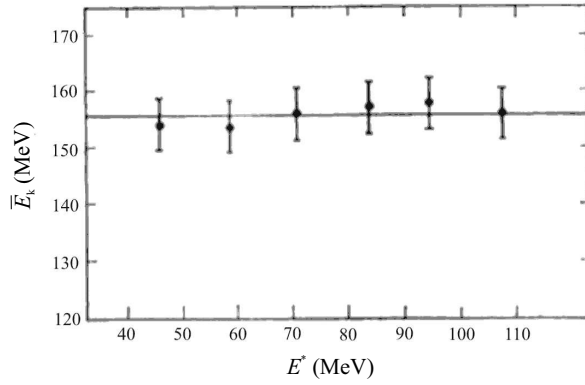


Fig. 6. The average kinetic energy vs the excitation energy of the compound nucleus formed in reaction  $^{16}\text{O}+^{209}\text{Bi}$  (from ref. [8])

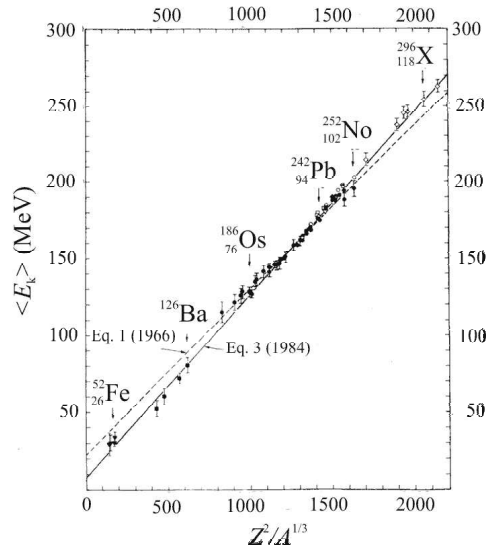


Fig. 7. The average kinetic energy vs  $Z^2/A^{1/3}$  parameter of the fissioning nucleus (from ref. [7])

As was discussed in Sec. 2 the particles in the fission process can be emitted before (pre-scission) and after (post-scission) fission. It was shown in ref. [5] that the pre-scission and post-scission neutron multiplicities  $M_{\text{pre}}$ ,  $M_{\text{post}}$ , respectively, depend on the excitation energy of the compound nucleus  $E^*$  (Fig. 5) as follows:

$$M_{\text{pre}} = (E^*/50\text{MeV}) + 1.6, \quad (5)$$

$$M_{\text{post}} = (E^*/200\text{MeV}) + 3. \quad (6)$$

The pre-scission neutron multiplicity increases with the excitation energy while the post-scission neutron multiplicity is almost constant. Most of the excitation energy of the highly excited composite nuclei is removed by evaporation of pre-scission neutrons. Thus the fissioning nucleus is rather cold at the moment of scission and its excitation energy is independent on the initial excitation energy [6].

A systematic study of the fission fragments average kinetic energy ( $\bar{E}_k$ ) was completed by Viola [7]. It was shown that  $\bar{E}_k$  depends on the Coulomb parameter  $Z^2/A^{1/3}$ , i.e. the average kinetic energy depends on the Coulomb repulsion force and does not depend on the excitation energy of the fissioning nucleus (see Fig. 6). Thus the average kinetic energy in MeV (Fig. 7) is:

$$\bar{E}_k = (0.1189 \pm 0.0011)Z^2/A^{1/3} + 7.3(\pm 1.5). \quad (7)$$

The highest angular momentum observed in the fission fragments from spontaneous fission is about  $16 \hbar$  [9]. The maximum angular momentum of the fission fragments obtained in heavy-ion induced fission reaction is again about  $16 \hbar$  [10]. It was suggested that this limitation on the observed angular momentum is due to the Doppler effect [11]. The half-life of the highest-spin states in the mass region reached by fission perhaps is very short, so the nucleus de-excites in flight.

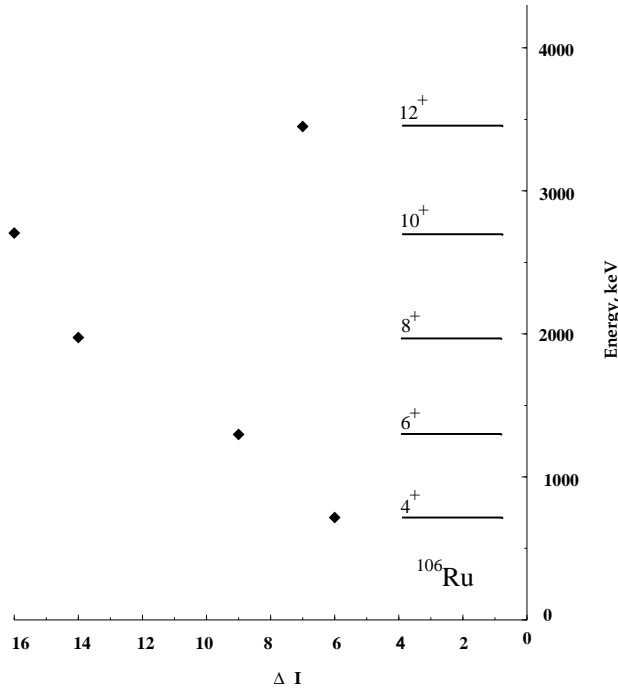


Fig. 8.  $\Delta I$  as a function of the energy in  $^{106}\text{Ru}$  (data taken from ref. [11])

Experimental study on the relative intensity is discussed in ref. [11]. A relationship between the feeding (measured by the sum of  $\gamma$ -ray intensities  $I_{in}(I)$  feeding

the particular level at angular momentum  $I$ ) and the de-excitation (measured by the  $\gamma$ -ray intensities  $I_{\text{out}}(I)$  de-excite the same level  $I$ ) of each yrast state in  $^{106}\text{Ru}$  was observed (see Fig. 8). It was shown that the maximum value of  $\Delta I = I_{\text{out}} - I_{\text{in}}$  is about  $10 \hbar$  which indicates that non-yrast but parallel to the yrast band states remain unobserved.

#### 4. EXPERIMENT

As it was discussed earlier the induced fission produces two fragments of equal  $Z/A$  ratio which is the same as for the compound nucleus. Thus if one wants to produce the nuclei  $^{108,110}\text{Pd}$  the  $Z/A_p$  ratio for the compound nucleus has to be chosen equal to 0.42–0.43 which is its value for these fission fragments. The reaction in our experiment was  $^{31}\text{P} + ^{176}\text{Yb}$  at beam energy of 152 MeV. In order to reduce the neutron emission probability the bombarding energy was chosen to be slightly above the Coulomb barrier. Following eq. (4) it has to be about 122 MeV. The  $^{31}\text{P}$  ions were accelerated by the VIVITRON accelerator at IReS, Strasbourg. A  $1.5 \text{ mg/cm}^2$  target of  $^{176}\text{Yb}$  was used onto which a Au layer of  $15 \text{ mg/cm}^2$  had been evaporated in order to stop the recoiling nuclei, thus to reduce the Doppler effect.  $\gamma$ -rays were detected with the EUROBALL4 multidetector array. The data were recorded in event-by-event mode with requirement that a minimum of three unsuppressed Ge detectors fired in prompt coincidence. A total of  $2.2 \times 10^9$  coincidence events were collected:  $1.2 \times 10^9$  are three-fold,  $6 \times 10^8$  four-fold,  $2.4 \times 10^8$  five-fold.

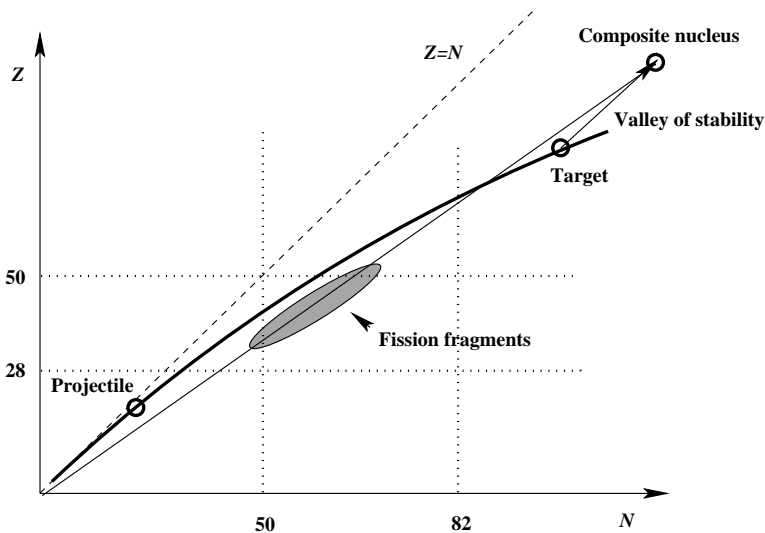


Fig. 9. Valley of stability and the populated from a fusion/fission reaction region

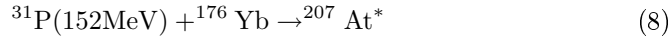
About eighty nuclei were produced as fission fragments (FF). The reached mass region extends from Ni to Ba along the valley of stability and beyond it towards the neutron-rich side. The most populated nuclei in our experiment are the Mo-Tc pair of complementary FF corresponding to a symmetric fission of the odd- $Z$  compound nucleus  $^{207}\text{At}$ . In this experiment  $^{108}\text{Pd}$  and  $^{110}\text{Pd}$  are nearly equally populated which gives  $\sim 10\%$  higher population for  $^{108}\text{Pd}$  and  $\sim 30\%$  for  $^{110}\text{Pd}$  in comparison with the previous experiment [10]. In all cases of complementary fragments  $Z_1 + Z_2 = 85$ , indicating that the proton evaporation in fission channel is highly suppressed.

**Table 1.** Average mass number before and after emission of post-scission neutrons  $A$  and  $A_p$ , respectively, and  $Z/A_p$  ratio for the produced nuclei (from ref. [11])

Element	average $A$	$A_p$	$Z/A_p$
$^{40}\text{Zr}$	94.1	96.1	0.42
$^{42}\text{Mo}$	99.2	101.2	0.42
$^{44}\text{Ru}$	104.2	106.2	0.41
$^{46}\text{Pd}$	108.6	110.6	0.42
$^{48}\text{Cd}$	113.7	115.7	0.41

The experimentally measured average mass numbers before and after the emission of post-scission neutrons ( $A$  and  $A_p$ ) for Zr, Mo, Ru, Pd and Cd isotopic chains are given in Table 1. Conservation of  $Z/A_p$  ratio is observed. As a result from the observed symmetric fission the  $Z/A_p$  ratio for  $^{205}\text{At}$  compound nucleus is the same as for the fission fragments.

The conservation of the energy and momenta for the reaction



gives:

$$E_0^{\text{P}} + E_{\text{kin}}^{\text{P}} + E_0^{\text{Yb}} = E_{\text{kin}}^{\text{At}} + E_0^{\text{At}} + E_{\text{At}}^* \quad (9)$$

$$\vec{P}_{\text{P}} = \vec{P}_{\text{At}}. \quad (10)$$

Thus the kinetic energies of  $^{31}\text{P}$  and  $^{207}\text{At}^*$  are 10% and 1.8% from the speed of light, respectively.

The excitation energy of the compound nucleus  $^{207}\text{At}$   $E^*(^{207}\text{At})=67.55$  MeV can be obtained taking into account the mass excess  $\Delta$  of the nuclei that  $Q = \Delta(\text{P}) + \Delta\text{Yb} - \Delta\text{At} = -21.441 - 53.497 + 13.25 = -61.688$ . As was discussed above, the proton evaporation channel is highly suppressed when the fission process occurs, therefore the complementary fragments of  $^{46}\text{Pd}$  isotopes in the  $^{207}\text{At}$  fission channel are  $^{39}\text{Y}$  isotopes ( $Z'_1 + Z'_2 = 84$ ). Each Pd isotope has complementary

fragments of different  $A$ , which have Gaussian distribution over some average  $A$ -value. After the emission of one to 5 neutrons the compound nucleus excitation energy decreases from 58.71 MeV to 24.71 MeV. The neutron binding energies are shown in Table 2.

**Table 2.** Neutron binding energies  $S_n$  in MeV for some compound nuclei (CN) and some complementary fission fragments (FF1, FF2)

CN	$S_n$	FF1	$S_n$	FF2	$S_n$
$^{207}\text{At}$	8.84	$^{114}\text{Pd}$	12	$^{94}\text{Y}$	6.18
$^{206}\text{At}$	7.55	$^{113}\text{Pd}$	5.43	$^{93}\text{Y}$	7.49
$^{205}\text{At}$	9.21	$^{112}\text{Pd}$	11.34	$^{92}\text{Y}$	6.55
$^{204}\text{At}$	7.68	$^{111}\text{Pd}$	5.75	$^{91}\text{Y}$	7.93
$^{203}\text{At}$	9.56	$^{110}\text{Pd}$	10.63	$^{90}\text{Y}$	6.86
$^{203}\text{At}$	9.56	$^{109}\text{Pd}$	6.15	$^{89}\text{Y}$	11.48

After the emission of several neutrons



the compound nucleus will fission into two fragments



It follows from the energy conservation law that

$$E_{\text{At}}^* + E_{0,\text{At}} = E_{\text{Pd}}^* + E_{0,\text{Pd}} + E_{\text{kin,Pd}} + E_{\text{Y}}^* + E_{0,\text{Y}} + E_{\text{kin,Y}} \quad (13)$$

and taking into account that the total kinetic energy ( $TKE$ ) of both fragments depends only on the Coulomb repulsion force between them one obtains

$$TKE = E_{\text{kin,Pd}} + E_{\text{kin,Y}} = 0.12 \frac{Z^2}{A} + 7.3 \sim 154.5 \text{ MeV} . \quad (14)$$

Thus the excitation energy of both fragments will be

$$E_{\text{Pd}}^* + E_{\text{Y}}^* = E_{\text{At}}^* + Q + TKE . \quad (15)$$

The excitation energy for some Pd and Y isotopes has been calculated supposing that the excitation energy of the compound nucleus is distributed over both fragments. Their respective excitation energies are given in Table 3. These values are high enough for neutron evaporation.

The calculated maximum value of the total number of emitted (pre-scission and post-scission) neutrons in our reaction is 8, but the neutron kinetic energy is not taken into account. Thus the calculated neutron multiplicity is consistent with that measured in ref. [5].

**Table 3.** Several fission reaction channels

CN	FF1	FF2	emitted neutrons
$^{205}\text{At}$	$^{114}\text{Pd}$ (29.9 MeV)	$^{91}\text{Y}$ (23.8 MeV)	5
	$^{112}\text{Pd}$ (29.8 MeV)	$^{93}\text{Y}$ (24.7 MeV)	6
	$^{110}\text{Pd}$ (28.7 MeV)	$^{95}\text{Y}$ (24.8 MeV)	6
$^{204}\text{At}$	$^{114}\text{Pd}$ (25.3 MeV)	$^{90}\text{Y}$ (20.0 MeV)	4
	$^{112}\text{Pd}$ (25.3 MeV)	$^{92}\text{Y}$ (20.8 MeV)	4
	$^{110}\text{Pd}$ (24.3 MeV)	$^{94}\text{Y}$ (20.8 MeV)	4
$^{203}\text{At}$	$^{114}\text{Pd}$ (21.6 MeV)	$^{89}\text{Y}$ (16.8 MeV)	3
	$^{112}\text{Pd}$ (22.0 MeV)	$^{91}\text{Y}$ (17.9 MeV)	4
	$^{110}\text{Pd}$ (21.6 MeV)	$^{93}\text{Y}$ (28.3 MeV)	4

One can deduce how many neutrons have been emitted in this process by means of  $\gamma$ -ray emission, although in the experiment discussed here we could not determine how many are the emitted pre-scission and post-scission neutrons separately. However, the number of pre-fission and post-fission neutrons had been directly measured for several compound nuclei at various excitation energies. At excitation energy of 65 MeV  $^{210}\text{Po}$  emits about 3 neutrons before fission and each fragment emits over 1.7 neutrons, which is consistent with the observed number of evaporated neutrons in our experiment.

## 5. GAMMA-RAY SPECTROSCOPY OF FISSION FRAGMENTS

Three techniques have been used in the experimental data analysis:

- i) three-dimensional  $\gamma$ -matrices (“cube”) constructed by the RADWARE code package [12] for level scheme extension;
- ii) two-dimensional ( $4\text{K} \times 4\text{K}$ )  $\gamma$ - $\gamma$ -matrices (with and without energy condition) and multiple gated spectra constructed by the code FANTASTIC [13];
- iii) single gated spectra constructed from these matrices by the code “MAT+SPEC” [14] with various options for background subtraction.

The cube provides a rapid access to the data which contain  $\gamma$ -ray cascades from more than eighty fission fragments as well as from the strong non-fission channels of the compound nucleus (CN)  $^{207}\text{At}$ . The relative intensities had to be obtained from high-fold events due to overlapping of transition energies belonging to different reaction products.

In comparison with the usual  $\gamma$ -ray spectroscopy of CN or its evaporation channel reactions when only a few nuclei are produced the  $\gamma$ -ray fission fragment (FF) spectroscopy has some particular difficulties:



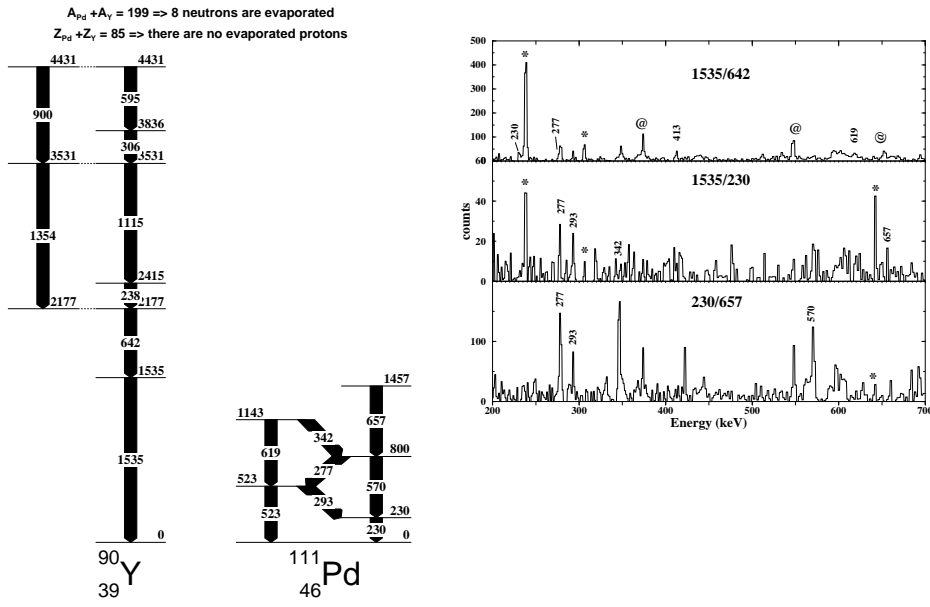


Fig. 11. Coincidence spectra obtained by double gating in  $^{90}\text{Y}$  and the candidates in  $^{111}\text{Pd}$  [15]. The transitions marked with stars belong to  $^{90}\text{Y}$  and those marked with @ to  $^{110}\text{Pd}$

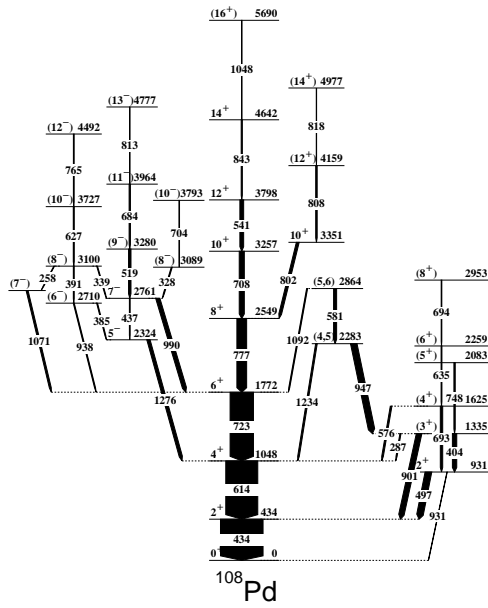


Fig. 12. Level scheme of  $^{108}\text{Pd}$  (from ref. [22])

For a particular transition in nucleus  $(A_1, Z_1)$  we can deduce the mean mass of the complementary fragments  $A_2$  that accompany it using the relative yields of the observed complementary fragments.

In the  $^{31}\text{P}+^{176}\text{Yb}$  reaction, where the compound nucleus is  $^{207}\text{At}^*$  the complementary fragments of  $^{110}\text{Pd}$  are several Y isotopes. Thus the spectra conditioned on the low-lying transitions in  $^{90}\text{Y}$  for example will contain the most intensive transitions in  $^{110}\text{Pd}$  and its neighboring Pd isotopes (Fig. 10). Gating on transitions in  $^{110}\text{Pd}$  and  $^{90}\text{Y}$  the yrast band in  $^{110}\text{Pd}$  could be obtained.

The identification method based on prompt coincidence between  $\gamma$ -rays emitted by complementary fragments has been applied initially for spontaneous fission [16] and recently confirmed for heavy-ion induced fission [17]. This method has successfully been used before this study for search of the unfavored band in  $^{109}\text{Pd}$  based on 98 keV transition [18].

The same procedure has been applied for searching the positive-parity bands in odd- $^{109,111}\text{Pd}$  nuclei [15]. The low-lying yrast states with positive parity in  $^{111}\text{Pd}$  are known from  $\beta$ -decay: the level at 230 keV and the 293 keV transition. The lowest-lying yrast state at 230 keV was found in spectra gated on the  $^{90}\text{Y}$  transitions. The search for these states started by examining various spectra conditioned on the presence of 230 keV transition and the transitions of the complementary Y isotopes  $^{90,91,92}\text{Y}$  (see Fig. 11). Then the spectrum gated on 230 keV transition and 1535 keV transition in  $^{90}\text{Y}$  was studied. In order to decide whether the new-found transitions belong to the Pd isotopes or to the complementary fragment  $^{90}\text{Y}$  other gates were used too. Finally, making spectra on some candidate line gave strong yrast state which belongs to the Pd isotopes under investigation and less intensive transitions from its complementary fragments.

## 6. RESULTS FOR $^{108,110}\text{Pd}$

The high-spin states in  $^{108}\text{Pd}$  have recently been studied via charged particle- $\gamma$  coincidences [19] and using a deep inelastic reaction [20]. The yrast band was observed up to  $I^\pi = 16^+$  and the even parity side band up to  $I^\pi = (14^+)$ . A negative parity band starting at the level 2324 keV has been established to  $I^\pi = (13^-)$ . The low-spin members of the  $\gamma$ -band have been studied by heavy-ion Coulomb excitation [21].

The level scheme of  $^{108}\text{Pd}$  obtained from our analysis is presented in Fig. 12 [22]. The transition intensities relative to the intensity of 723 keV transition are presented in the level scheme by the thickness of the vertical arrows. Coincidence spectra supporting the new extension of the level scheme are shown in Fig. 13.

The level scheme obtained for  $^{110}\text{Pd}$  is presented in Fig. 14. Examples of coincidence spectra are shown in Fig. 15.

In the present work the yrast positive-parity band is observed up to  $I^\pi = (14^+)$  beyond the first backbending in agreement with ref. [23] and a decay of the  $12^+$  state to the  $(10_2^+)$  state at 3196 keV has been identified. The quasi- $\gamma$  band is extended above the known  $3^+$  and  $4^+$  members up to the  $5^+$  and  $8^+$  levels.

A new structure, similar to the negative-parity bands observed in  $^{112}\text{Pd}$  [24], has been identified and several transitions linking it to the yrast band were found.

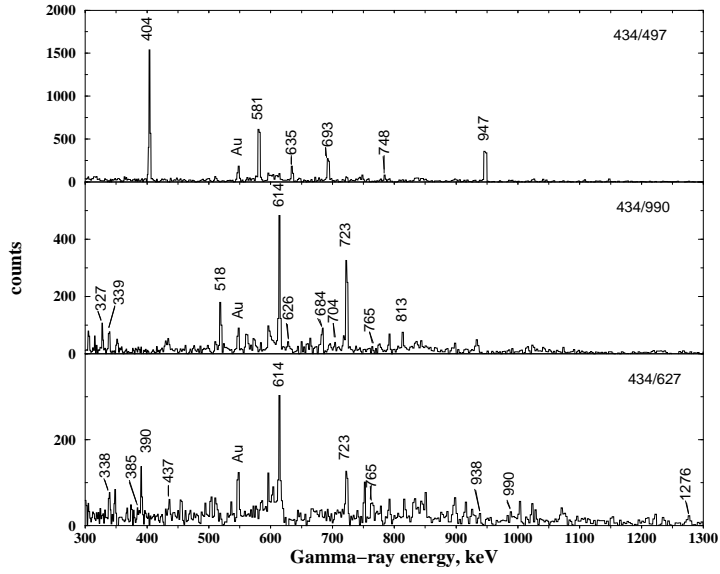


Fig. 13. Coincidence spectra obtained by double gating in  $^{108}\text{Pd}$  (from ref.[22])

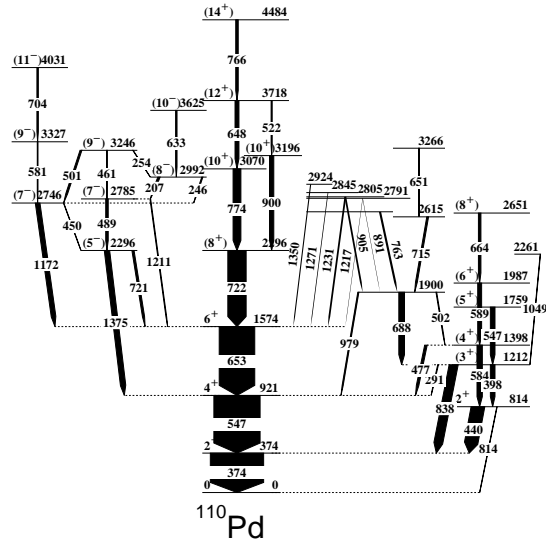


Fig. 14. Level scheme of  $^{110}\text{Pd}$  (from ref. [22])

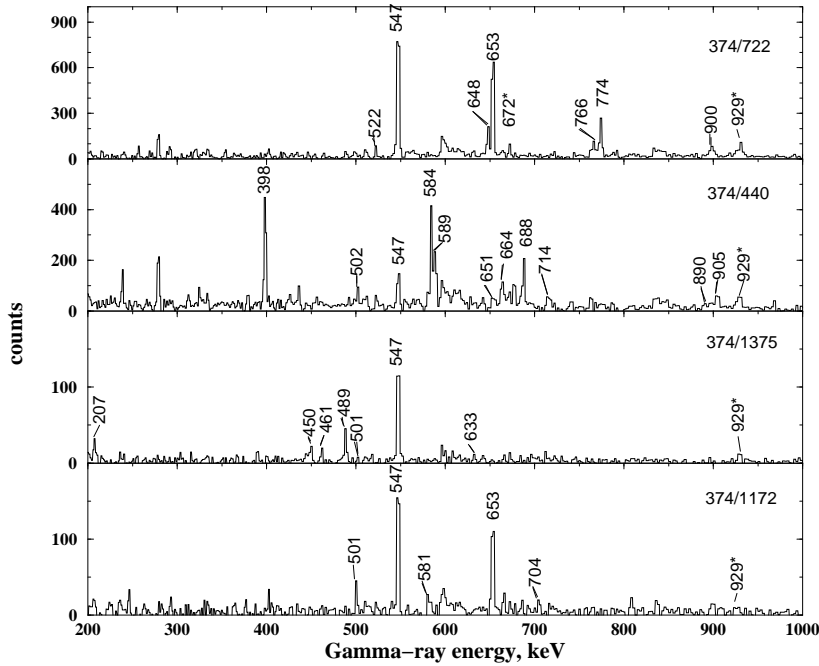


Fig. 15. Coincidence spectra obtained by double gating in  $^{110}\text{Pd}$ . The transitions marked with stars belong to the complementary fragment (from [22])

The statistics in our FF  $\gamma$ -ray experiment is not high enough to perform angular correlation analysis. The spin values in both  $^{108}\text{Pd}$  and  $^{110}\text{Pd}$  have been tentatively assigned on the basis of

- i) already known spins of band head states;
- ii) the usual assumption of increasing spin with the excitation energy for yrast population in the fission process;
- iii) systematics.

All the details about the new observed structures in  $^{108,110}\text{Pd}$  and their interpretation are given in ref. [22].

## 7. CONCLUSION

The aim of this work is to give an overview on heavy ion reactions: formation and decay of the compound nucleus and reactions of induced fission and also details on the fission process. On the basis of our experiment the details of fission fragment gamma-ray spectroscopy are explained and finally some results on Pd isotopes are shown.

**Acknowledgements:** This study is completed in the framework of an agreement between the University of Sofia and the University of Paris-Sud, Orsay (France) and in the framework of CNRS-Bulgarian Academy of Science agreement, project 9545. The authors would like to thank Dr M-G Porquet from CSNSM, Orsay, France, for introducing them to  $\gamma$ -ray fission fragment spectroscopy and for the very useful and elucidating discussions.

#### REFERENCES

1. Hodgson, P. E., E. Gadioli, and E. Gadioli Erba. *Introductory Nuclear Physics*, Clarendon Press, Oxford, 1997.
2. Wilczinski. *Nucl. Phys.* **A216**, 1973, 386.
3. Ejiri, H., and M.J.A. de Voigt. *Gamma-Ray and Electron Spectroscopy in Nuclear Physics*, Clarendon Press, Oxford, 1989.
4. Leigh, J. R. et al. *Phys. Rev. Lett.* **48**, 1982, 527.
5. Schröder, W. U. et al. *Nucl. Phys.* **A502**, 1989, 473.
6. Hinde, D. J. et al. *Nucl. Phys.* **A502**, 1989, 497.
7. Viola, V. E., K. Kwiatkowski, M. Walker. *Phys. Rev.* **C31**, 1985, 1550.
8. Viola, V. E. and T. Sikkerland. *Phys. Rev.* **130** v5, 1963, 2044.
9. Hamilton, J. H. et al. *Eur. Phys. J.* **A15**, 2002, 175.
10. Deloncle, I. et al. *Eur. Phys. J.* **A8**, 2000, 177.
11. Porquet, M.-G. et al. *Rapport d'activité*, CSCNSM 2001-2002.
12. Radford, D. C. *Nucl. Instrum. Methods Phys. Res.* **A361**, 1995, 297.
13. Deloncle, I., M.-G. Porquet, and Dziri-Marcé. *Nucl. Instrum. Methods Phys. Res.* **A357**, 1995, 150.
14. Deloncle, I. *Private communication*.
15. Porquet, M.-G. et al. *to be published*.
16. Hotchkins, M. A. C. et al. *Nucl. Phys.* **A530**, 1991, 111.
17. Porquet, M.-G. et al. *Acta Phys. Pol.* **B27**, 1996, 179.
18. Kutsarova, T. et al. *Phys. Rev.* **C58**, 1998, 1966.
19. Pohl, K. R. et al. *Phys. Rev.* **C53**, 1996, 2682.
20. Regan, P. H. et al. *Phys. Rev.* **C55**, 1997, 2305.
21. Svensson, L. E. et al. *Nucl. Phys.* **A584**, 1995, 547.
22. Lalkovski, S. et al. *Eur. Phys. J.* **A18**, 2003, 589.
23. Houry, M. et al. *Eur. Phys. J.* **A6**, 1999, 43.
24. Krücken, R. et al. *Eur. Phys. J.* **A10**, 2001, 151.

Stephane Lalkovski  
St. Kliment Ohridski University of Sofia  
Faculty of Physics  
Department of Atomic Physics  
5, James Bourchier Blvd.  
1164 Sofia, Bulgaria  
E-mail: stl@phys.uni-sofia.bg

*Received May 2004*